Mon. Not. R. Astron. Soc. **000**, 1–15 () Printed 23 July 2014 (MN LATEX style file v2.2)

First detection and characterization of symbiotic stars in M31

Joanna Mikołajewska[1⋆], Nelson Caldwell[2], Michael M. Shara[3]
[1]*N. Copernicus Astronomical Center, Bartycka 18, PL 00–716 Warsaw, Poland*
[2]*Harvard-Smithsonian Center for Astrophysics, Cambridge, MA 02138, USA*
[3]*Department of Astrophysics, American Museum of Natural History, Central Park West at 79th Street, New York, NY 10024, USA*

arXiv:1406.3080v3 [astro-ph.SR] 22 Jul 2014

Accepted Received

ABSTRACT
Symbiotic binaries are putative progenitors of type Ia supernovae. The census of Galactic symbiotic binaries is so incomplete that we cannot reliably estimate the total population of these stars, and use it to check whether that number is consistent with the observed type Ia supernova rate in spiral galaxies. We have thus begun a survey of the nearest counterpart of our own Galaxy, namely M31, where a relatively complete census of symbiotic stars is achievable. We report the first detections and spectrographic characterizations of 35 symbiotic binaries in M31, and compare these stars with the symbiotic population in the Milky Way. These newly detected M31 symbiotic binaries are remarkably similar to galactic symbiotics, though we are clearly only sampling (in this feasibility study) the most luminous symbiotics in M31. We have also found, in M31, the symbiotic star (M31SyS J004233.17+412720.7) with the highest ionization level known amongst all symbiotics. An optical outburst of the M31 symbiotic star M31SyS J004322.50+413940.9 was probably a nova-like outburst, the first symbiotic outburst detected outside the Milky Way and Magellanic Clouds.

Key words: surveys – binaries: symbiotic – planetary nebulae: general – M31

1 INTRODUCTION

1.1 Motivation

While not a single progenitor of a SNIa has been observed before the explosion, there is a consensus that these supernovae result from the thermonuclear disruption of Carbon-Oxygen white dwarfs (CO-WDs) reaching the Chandrasekhar mass (Paczynski 1985; Webbink 1994; Iben & Tutukov 1984). This must be due to either 1) rapid mass accretion onto a WD from a non-degenerate companion (single-degenerate or SD model); or 2) mass transfer between and/or merger of two WDs (double-degenerate or DD model). Each of the proposed scenarios has its strengths and weaknesses (Di Stefano et al. 2013, and references therein). Two particularly well-observed SNIa (in M101 Li et al. 2011; and in the LMC Schaeffer & Pagnotta 2012) almost certainly were of the DD type. A third SN Ia with hydrogen in its late spectrum was likely a symbiotic star of the SD type (Dilday et al. 2012).

Some SD binaries that are currently symbiotic stars (hereafter SySt) must inevitably evolve into DD systems (e.g. Di Stefano 2010; Mikołajewska 2013). Symbiotic stars are thus potential SD supernovae **and** the progenitors of DD supernovae.

SySt are amongst the longest orbital period interacting binaries. The components are an evolved cool giant and an accreting, hot, luminous companion (usually a WD) surrounded by a dense ionized nebula. Depending on the nature of the cool giant, two main classes of symbiotic stars have been defined. The S-types (stellar) are normal M giants with orbital periods of the order of a few years (see e.g. Mikołajewska 2012, and references therein). The D-types (dusty) contain Mira variable primaries surrounded by warm dust (Whitelock 1987); orbital periods are decades or longer (e.g. Schmid & Schild 2002; Gromadzki & Mikołajewska 2009). In addition to ionized and neutral regions, accretion/excretion discs, interacting winds, dust-forming regions, and bipolar outflows with jets are observed (see e.g. Mikołajewska 2007, 2012, for recent reviews). Some SySt must give rise to nova explosions (Yaron et al. 2005; Shara et al. 2010). Thus, in addition to their importance as SNIa progenitors, symbiotic stars offer insight into all interacting binaries that include evolved giants and accreting WDs during any phase of their evolution.

Only ~300 SySt are known today – mostly in the Milky Way, where our sample is very incomplete. This incompleteness is due to the lack of deep, all-sky surveys at wavelengths where SySt distinguish themselves from all other stars. As an example, there is no publicly-available, deep Hα survey at most moderate and high Galactic latitudes; nor is there a deep Brackett-gamma imaging survey of the Galactic Plane.

Why should we hunt for more, particularly in external galaxies? The most important reasons to acquire large, complete samples of extragalactic SySt are

(i) to enable a direct comparison of symbiotic total numbers in

⋆ E-mail: mikolaj@camk.edu.pl

© RAS

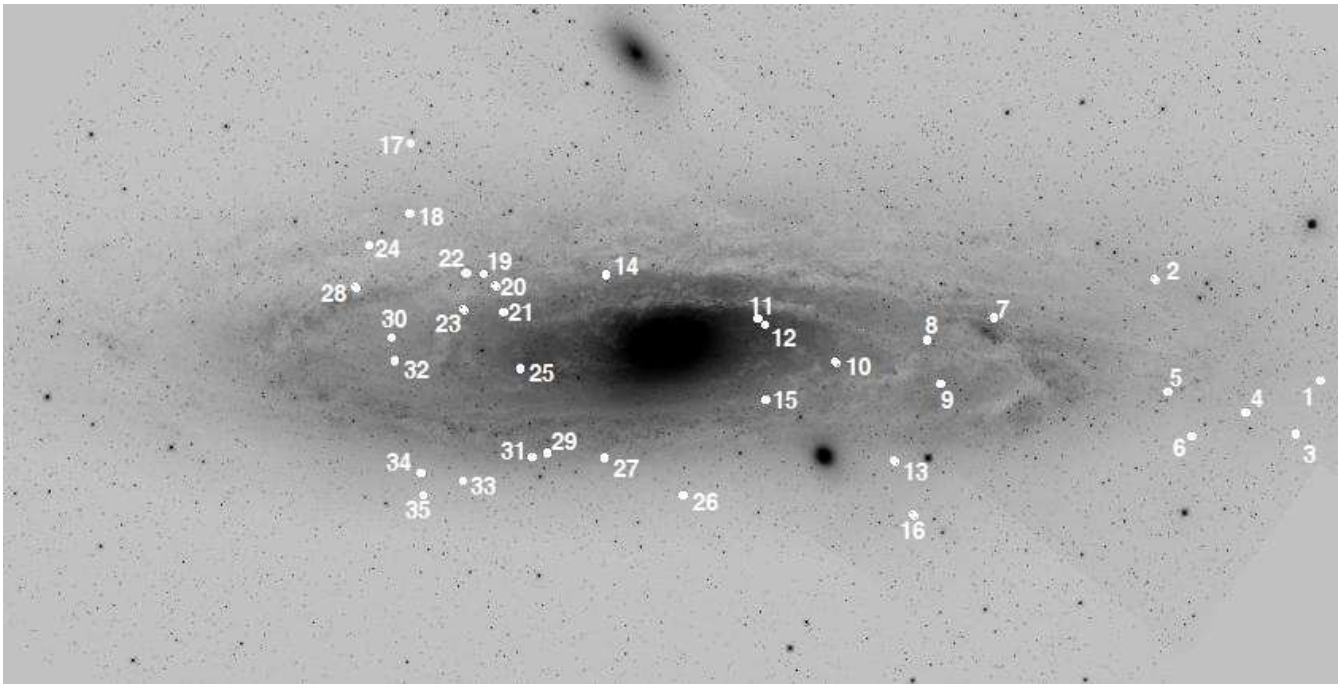

Figure 1. The distribution of M31 SySt and possible SySt, identified by their ordinal numbers in Table 1, and overlaid on the DSS optical image of M31. The field of view is $2.^\circ66 \times 1.^\circ27$.

galaxies with the numbers expected in these galaxies if SySt are SNIa progenitors;

(ii) to enable the spatial distributions of SySt in galaxies to be delineated, relative to the spiral arms and massive-star formation regions in each galaxy, for comparison with SNIa in spiral galaxies;

(iii) to eventually enable the characterization of a SySt **before** its eruption as an SNIa, a major confirmation of a prediction of binary stellar evolution theory.

Current estimates of the population of Milky Way SySt vary from 3,000 (Allen 1984), to 30,000 (Kenyon et al. 1993a) up to 400,000 (Munari & Renzini 1992; Magrini et al. 2003). However, fewer than 300 SySt have been detected in the Milky Way, and a few dozen more in the closest galaxies (e.g. Belczyński et al. 2000; Corradi 2012, and references therein; Miszalski et al. 2013 , 2014; Miszalski & Mikołajewska 2014; Goncalves et al. 2008; Kniazev et al. 2009; Oliveira et al. 2013).

Hakobyan et al. (2011) demonstrated that a significant fraction of SNIa in spiral galaxies preferentially occur in young, star-forming regions. If SySt are associated with SNIa, then they, too, should show some preference for the spiral arms and HII regions in spiral galaxies. All existing surveys for SySt are so badly incomplete that we can say nothing about their global populations in any other galaxy. We are equally ignorant of the global spatial distribution of SySt in the Milky Way. This paper is a demonstration of feasibility of acquiring a complete census of the SySt in the Local Group of galaxies, and a first step in tracing the locations of SySt in M31.

If SySt (or some subset of all SySt) are really the progenitors of SNIa, then eventually one of these objects will erupt in a Local Group galaxy (including the Milky Way). The larger the sample of spectrographically confirmed SySt (in any galaxy) that astronomers will have, the greater the possibility that one of these SySt will be the progenitor. It is thus clear that a sample of **at least** 10 000 SySt is required to have a reasonable chance of observing one erupt during an astronomer's lifetime. This would be an enormous success for stellar evolution theory.

1.2 Why M31?

With these motivations in mind, we have begun a concerted search for extragalactic SySt. The powerful Hα emission of SySt is as distinctive in halo and extragalactic stars as in their local counterparts. SySt are simultaneously very blue (in U–B colours) and very red (in V–I colours), due to the simultaneous presence of a very hot white dwarf and and cool red giant. Thus a large survey for extragalactic SySt should be based on a survey with (at least) $UBVI$ and Hα magnitudes for a large number of extragalactic stars.

At first glance the logical galaxies to start with are the LMC and SMC. They certainly are the closest major Local Group members, and a few SySt have been detected in each. The strongest drawbacks to these galaxies are their apparent sizes and lack of suitable databases. About 150 square degrees would have to be surveyed to fully cover the LMC and SMC. No suitably deep, well-resolved, publicly available $UBVI$Hα atlases or catalogs of the LMC and SMC exist.

Fortunately there **is** a large, deep, uniform, well-calibrated and documented, publicly-available $UBVI$Hα (as well as [O III] and [S II]) survey and catalog of nine other Local Group galaxies that is ideal for our purposes. Massey et al. (2006) used 42 nights of the KPNO and CTIO 4 meter telescopes, Mosaic cameras and the Lowell Observatory 1.1 meter telescope to exhaustively image, calibrate and catalog the galaxies M31, M33, IC10, NGC 6822, WLM, Sextans A, Sextans B, Pegasus and Phoenix. Careful astrometry was used to ensure stellar positions accurate to 0.2 arcsec. Painstaking photometric calibrations of each CCD chip assured 3 per cent photometry at $U \sim B \sim V \sim R \sim I \sim 22$, and as faint as H$\alpha \sim 21$. This corresponds well to the magnitudes expected for SySt in these galaxies. It also ensures colours accurate to better than 5 per cent.

Massey et al focused (successfully) on a search for Luminous Blue Variables in their nine galaxies. The LGGS catalog is freely available from the NOAO archives. It contains the positions, magnitudes and *UBVRI* colours of 518 000 stars in M31 and M33, and 88 000 stars in the other galaxies. One of us (NC) has already collected spectra of stars with strong Hα emission in M31 detected in LGGS, and it is the results of this spectrographic reconnaissance that we report in this paper.

In Sect. 2 we describe the data and their reductions. The coordinates and spectra of 35 new M31 SySt are presented in Sect. 3. We characterize these stars, and contrast and compare them with SySt in our own Galaxy in Sect. 4. A brief summary of our results is found in Sect. 5.

2 OBSERVATIONS AND DATA REDUCTION

The symbiotic stars discussed in this paper were found as "by-products" of a spectrographic survey of M31 aimed at detecting and characterizing HII regions and planetary nebulae (PNe)(Sanders et al (2012)). HII region candidates were chosen because they displayed strong Hα emission in images of the publicly-available LGGS (Massey et al. 2007). Planetary nebula candidates were chosen from the planetary nebula catalog of Merrett et al. (2006), as well as from strong and unresolved [O III] emission objects in the LGGS images. A second set of spectra was collected in 2011 (using the catalog of Azimlu et al. 2011), which also contained objects selected on the basis of Hα emission. In all, the spectra of about 700 objects which displayed Hα or [O III] emission were collected. About 95% of the candidates did turn out to be HII regions and PNe, as expected.

Upon visual inspection of all the spectra, we found that a small number of objects were neither PNe nor HII regions. While all display a strong Hα line, they have little or no emission in the familiar forbidden lines of [N II], [S II], and [O II]. Instead, they show lines of high ionization potential. These 35 objects, listed in Table 1, are the subject of this paper. We emphasize that none of these candidates were selected for spectroscopy with the expectation that they might be SySt. Any statistical analyses of the SySt in M31, based on this sample alone, should take this into consideration.

The spectra themselves were obtained with the Hectospec multi-fiber positioner and spectrograph on the 6.5m MMT telescope (Fabricant et al. 2005), as described in Caldwell et al. (2009). The Hectospec 270 gpm grating was used and provided spectral coverage from roughly 3700 – 9200Å at a resolution of ∼ 5Å. Some spectra did not cover [O II]λ3727, because of the design of the spectrograph, and the small blueshift of M31. The observations were made in the period from 2004–2007 and 2011, and were reduced in the uniform manner outlined in Caldwell et al. (2009). The frames were first de-biased and flat fielded. Individual spectra were then extracted and wavelength calibrated. Sky subtraction is achieved with Hectospec by averaging spectra from "blank sky" fibers from the same exposures or by offsetting the telescope by a few arcseconds. Standard star spectra obtained intermittently were used for flux calibration and instrumental response. These relative flux corrections were carefully applied to ensure that the relative line flux ratios would be accurate. The total exposures were between 1800 and 4800s.

16 of our targets have LGGS photometry (Massey et al. 2006) and their *UBVI* are collected in Table 2. The uncertainty on individual measurements is less than 0.03 mag for objects brighter than ∼ 22 mag, and 0.1–0.3 for the fainter ones. Since Massey et al. (2006) required a detection in all filters for inclusion in their catalog, very red stars are left out. So, additional *I* photometry from the LGGS was obtained for most of the candidates that were not in Massey et al.'s catalog. These *I* magnitudes (Table 2) were obtained by measuring aperture photometry of stars in relevant mosaicked images, cross-correlating those stars with ones actually in the Massey catalog, deriving a transformation, and then applying that transformation to the measurements of the missing stars. The estimated errors are around 0.3 mag for these. Three objects, M31SyS J004059.40+405003.1, M31SyS J004358.20+412850.9, and M31SyS J004349.54+413855.9, were too faint to be measured using this technique, though they do show up in the *I* band images.

The PHAT survey (Dalcanton et al. 2012) has imaged the NE half of the disk of M31 in 6 filters from the UV to the near IR, thus approximately half of our SySt sample lies within that survey. Details of the point-spread function fitting photometry are contained in Williams et al. (2014). What we have done is search the PHAT photometric catalogs for coordinate matches with our SySt candidates. Since the fiber aperture is 1.5 arcsec in diameter, we allowed a tolerance of 0.75 arcsec in the coordinate matching. Of the 10–20 stars in the catalog within that coordinate tolerance, we chose the star with the brightest F814W magnitude to be the SySt. Typically, the brightest star was more than 1 magnitude brighter than the next brightest, so it seems safe to assume we have chosen the correct star. Of the 11 SySts with PHAT photometry, only one proved to be problematic, with several stars of similar magnitude within the fiber aperture. We do not report values for this case.

Table 2 also gives the 2MASS *JHK* photometry for some of our objects. The locations of all of our targets in M31 are displayed in Fig. 1.

3 IDENTIFICATION AND CLASSIFICATION OF SySt IN M31

The optical spectra of SySt are characterized by the presence of absorption features and continua appropriate for a late-type M giant, and strong nebular emission lines of Balmer H I, He II, He I, He II and forbidden lines of [O III], [Ne III], [Ne V], and [Fe VII]. Optical spectra of large samples of SySt were catalogued by Allen (1984) and Munari & Zwitter (2002). The spectra of many SySt also show a broad emission feature at about λ6830 Å, and a factor of ∼ 4 weaker but similar feature at about λ7088 Å. Allen (1980) found that ∼ 50 per cent SySt exhibit this band. He also found that the λ6830 Å feature is only observed in SySt. Schmid (1989) first identified the $\lambda\lambda$6830, 7088 lines as Raman scattering of the O VI resonance lines $\lambda\lambda$1032, 1038 by neutral hydrogen. The proposed production mechanism of these features confirms their intrinsic connection with the interaction between the hot component (copious in O VI photons) and the cool component (with its strong stellar wind) of the SySt. Thus the presence of the Raman scattered lines provides a very strong criterion for the identification and classification of SySt.

The composition of SySt is also reflected by their broad-band colours. They appear blue in the UV, where the nebular line and continuum emission dominates the spectral energy distribution (SED), and red in the optical and near IR, because of the emerging red giant spectrum.

Table 1 gives the names and coordinates of 31 bona-fide and 4 possible SySt in M31 that were classified as such systems following the criteria in Mikołajewska et al. (1997) and Belczyński et al. (2000). According to the IAU recommendations,

Table 1. List of new and possible symbiotic stars with accurate coordinates, their other cross identifiers, and the reference to the number of figure presenting the spectrum

No.	M31SyS J	RA(2000)	DEC(2000)	LGGS J	[AMB2011]	CrossIDs	Fig.
1	003846.16+400717.0	00:38:46.159	40:07:16.995				A1
2	003857.17+403132.2	00:38:57.166	40:31:32.216	003857.19+403132.2	106		A1
3	003923.79+400543.4	00:39:23.792	40:05:43.378	003923.80+400543.5			A1
4	003932.01+401224.7	00:39:32.010	40:12:24.708			SDSS9 J003931.98+401224.8	A1
5	003951.85+402153.8	00:39:51.847	40:21:53.773		407		A1
6	004005.96+401604.3	00:40:05.964	40:16:04.325			2MASS J00400597+401604	A1
7	004021.10+404501.1	00:40:21.096	40:45:01.085	004021.11+404501.2	575		A1
8	004059.40+405003.1	00:40:59.400	40:50:03.127		1022		A1
9	004117.11+404524.1	00:41:17.112	40:45:24.115	004117.09+404524.2	1172		A2
10	004147.71+405737.1	00:41:47.712	40:57:37.082		1418	[PAC]61099 M31N 1993-05	A2
11	004155.61+410846.7	00:41:55.608	41:08:46.685	004155.60+410846.7	1455	2MASS J00415562+4108487	A2
12	004156.21+410735.0	00:41:56.208	41:07:35.040		1458		A2
13	004216.70+404415.7	00:42:16.704	40:44:15.725	004216.72+404415.8	1586	2MASS J00421671+4044158 [PAC]57435 NBVF020684	A2
14	004233.17+412720.7	00:42:33.167	41:27:20.712		1681	2MASS J00423313+4127207	11
15	004235.59+410148.0	00:42:35.592	41:01:47.996		1693	[PAC]93855	A2
16	004237.49+403813.2	00:42:37.488	40:38:13.204	004237.49+403813.2	1696		A2
17	004241.96+415656.4	00:42:41.962	41:56:56.405				A2
18	004319.98+415137.5	00:43:19.976	41:51:37.540			NBW9012546	A3
19	004322.50+413940.9	00:43:22.495	41:39:40.875	004322.50+413940.9	2115	2MASS J00432249+4139409 BATC_004322.51+413941.1 M31V J00432248+4139408 [PAC]47174	12
20	004323.68+413733.6	00:43:23.682	41:37:33.557		2122	WISE J004323.68+413733.6 M31 J00432365+4137335 [PAC]47312	3
21	004334.79+413447.9	00:43:34.794	41:34:47.869	004334.78+413447.9	2270	M31V J00433475+4134477 [PAC]46291	A3
22	004335.01+414358.2	0:43:35.010	41:43:58.216		PN275		A3
23	004349.54+413855.9	00:43:49.543	41:38:55.886			M31 J00434953+413855	4
24	004353.59+415323.3	00:43:53.592	41:53:23.284		2478	NBW9056509 M31V J00435354+4153232	A3
25	004358.20+412850.9	00:43:58.200	41:28:50.882		2528	M31V J00435816+4128508	A3
26	004359.52+410253.5	00:43:59.517	41:02:53.515		2541		A3
27	004411.71+411336.0	00:44:11.713	41:13:35.994	004411.71+411336.1	2703	BATC J004411.66+411335.9 D31 J004411.7+4111335.9	2
28	004421.89+415125.6	00:44:21.891	41:51:25.648	004421.90+415125.7	2808	M31V J00442188_4151255	A3
29	004432.09+411940.8	00:44:32.094	41:19:40.769	004432.06+411940.6	2996	NBVE012366 2MASS J00443214+4119408	A3
30	004433.74+414402.8	00:44:33.741	41:44:02.789	004433.74+414402.7	3020	2MASS J00443374+4144032 M31 J00443372+4144026 D31 J004433.7+414403.0	A4
31	004440.50+412052.2	00:44:40.495	41:20:52.194		PN 339		A4
32	004445.03+414156.5	00:44:45.030	41:41:56.473	004445.02+414156.5		M31 J00444500+4141563	A4
33	004521.55+412557.3	00:45:21.554	41:25:57.339			M31 J00452155+4125571	A4
34	004534.07+413049.0	00:45:34.069	41:30:48.958	004534.04+413049.0	3609	M31V J00453405+4130487	A4
35	004545.41+412851.6	00:45:45.408	41:28:51.596	004545.34+412851.7	3699		A4

[AMB2011] XXXX - number in the catalog of HII regions in M31 (table 2; Azimlu et al. 2011)

[AMB2011] PNXXX - number in the catalog of PNe in M31 (table 3; Azimlu et al. 2011)

[PAC]... - POINT-AGAPE Catalogue identifier (An et al. 2004)

NW... - indentifier in The Guide Star Catalog Version 2.3.2 (GSC2.3; STScI, 2006)

BATC... - BATC Data Release One (Zhou et al. 1995–2005)

M31... - Vilardell et al. (2006)

D31... - DIRECT (Mochejska et al. 2001)

Table 2. Photometric data of new and likely new SySt

M31SyS J	LGGS					PHAT						2MASS		
	V	*B–V*	*U–B*	*V–I*	*I*	m_{275}	m_{336}	m_{475}	m_{814}	m_{110}	m_{160}	*J*	*H*	*K*
003846.16+400717.0					20.77									
003857.17+403132.2	20.85	0.31	-1.23	0.98										
003923.79+400543.4	21.00	0.32	-0.66	1.35										
004156.21+410735.0					20.37									
003951.85+402153.8					20.59									
004005.96+401604.3					19.76							18.3	16.6	16.75
004021.10+404501.1	23.03	0.98	-1.41	2.61										
004059.40+405003.1					$\gtrsim$21									
004117.11+404524.1	22.78	-0.06	-1.47	1.90										
004147.71+405737.1					20.47									
004155.61+410846.7	21.26	0.38	-0.84	1.40								16.5	16.01	15.1
004156.21+410735.0					20.54									
004216.70+404415.7	20.70	0.60	-0.32	1.31								18.05	17.9	16.8
004233.17+412720.7					19.77							16.82	15.88	15.50
004235.59+410148.0					20.48									
004237.49+403813.2	22.35	0.61	-0.44	1.05										
004319.98+415137.5					19.94									
004322.50+413940.9	20.35	0.84	-0.50	1.25								17.39	16.17	15.91
004323.68+413733.6					20.91									
004334.79+413447.9	20.91	0.39	-0.67	1.35		21.452	20.910	20.804	19.452	18.440	17.480			
004349.54+413855.9					$\gtrsim$ 21	21.410	21.330	23.066	20.487	18.915	17.879			
004353.59+415323.3					20.62									
004358.20+412850.9					$\gtrsim$21	26.408	23.973	23.954	21.056	19.373	18.269			
004359.52+410253.5					20.55									
004411.71+411336.0	20.81	0.77	-0.59	1.68		21.449	21.248	22.014	19.458	18.676	17.975			
004421.89+415125.6	21.27	-0.02	-0.84	1.36		27.562		22.366	20.327	18.571	17.588			
004432.09+411940.8	21.15	0.28	-0.08	0.44								17.2	15.9	15.46
004433.74+414402.8	21.57	0.36	-1.00	2.37		23.066	21.848	23.028	19.842	17.924	16.745	16.97	15.98	15.52
004440.50+412052.2						22.786	21.526	22.110	22.212	20.664	19.028			
004445.03+414156.5	22.35	-0.33	-0.31	1.95		21.404	21.256	22.448	21.401	18.086	17.301			
004521.55+412557.3						23.911	22.432	23.130	23.219	21.206	19.629			
004534.07+413049.0	20.89	0.50	-0.82	1.27		21.548	20.793	21.145	19.699	18.996	18.149			
004545.41+412851.6	20.05	0.63	-0.71	1.03	19.09									

the name was built from the object position and considering the observational angular resolution. The resulting format is M31 SyS JHHMMSSss+DDMMSSs where the acronym M31 SyS indicates that they are also SySt. The finder charts are available via dedicated web page created by one of us (NC)[1]. These adopted criteria include the following:

(a) Presence of absorption features of a late-type giant: in practice this means TiO, and sometimes VO bands.

(b) Presence of strong H I, He I emission lines, together with emission lines of ions with ionization potential (IP) of at least 30 eV (e.g. [O III]).

(c) Presence of the Raman scattered O VI λ6830 even if no features of the cool star are found.

Examples of the spectra presenting all the defining features of SySt are shown in Figs. 2–4 whereas the spectra for all remaining SySt presented in this study are shown in the Appendix A (available online). The last column of Table 1 also gives the reference number of the figure in which the spectrum is presented.

Unfortunately, since our spectra come from a fiber system, only a few of them had a 'local' background subtracted. Typically the background was far away (10–20 arcminutes). Thus, some spectra in the disk and bulge show features due to their surroundings. Good examples are M31SyS J004156.21+410735.0 and M31SyS J004155.61+410846.7, which shows bulge absorption features as well as the stars' emission lines. The absorption features can be mistaken for a single red giant star, complicating the SySt classification.

The symbiotic nature of these objects is also confirmed by their brightnesses in *I* and red *V–I* colours. In particular, they all are a few magnitudes brighter than the *I* mag predicted by their Hα fluxes and by assuming that their red/near IR emission is of nebular origin; whereas the presence of a bright, cool giant star is consistent with their observed red magnitudes.

The hot components of SySt often show strong optical outbursts characterized by the appearance of bright A- or F-type continuua, as well as strong H I as well as O I, [O I], Fe II, [Fe II], and other low-excitation emission lines. The stronger emission lines present more or less complex P Cyg structure, while the red giant bands are only visible in the red/infrared spectral range. In our M31 SySt sample, this could be the case of M31SyS J004322.50+413940.9 (Fig. 12, and Sect. 4.3). In the present study we classify some objects showing only a low-excitation nebular spectrum in addition to TiO bands in their red spectra as possible SySt.

Table 3 summarizes the spectroscopic characteristics of our sample, in particular, the selected emission line flux ratios, the high-

[1] http://www.cfa.harvard.edu/oir/eg/m31clusters/symb/symb.html

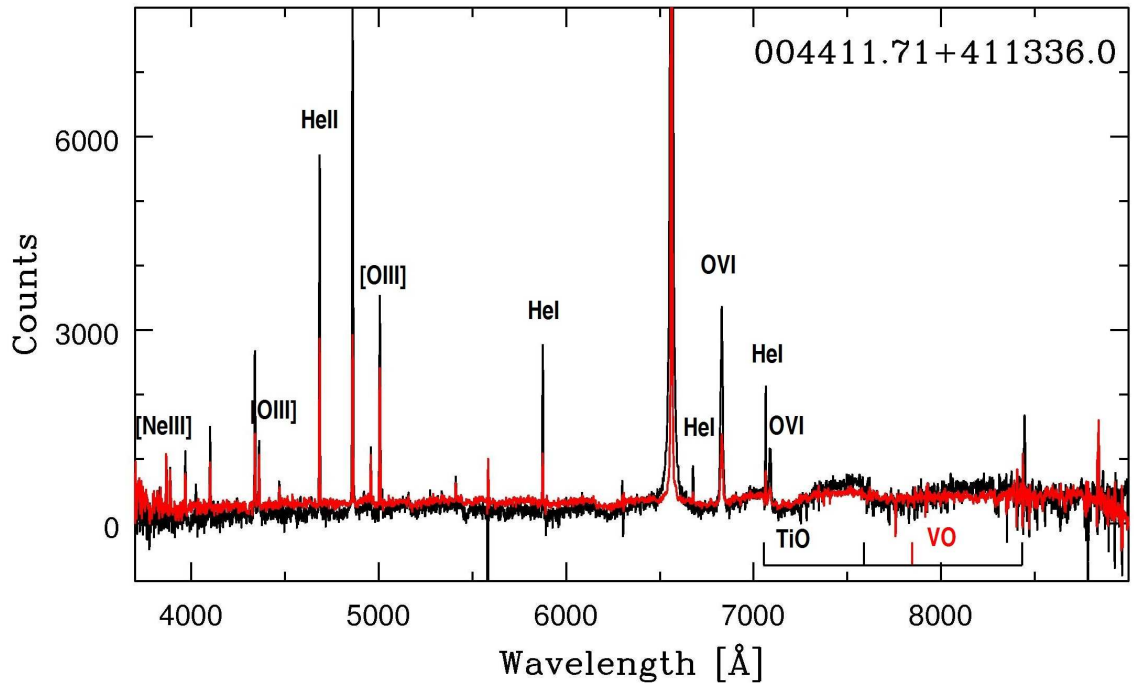

Figure 2. The spectrum of M31SyS J004411.71+411336.0 which presents all the defining features of a classical S-type SySt. The black and red colours correspond to the spectra taken in 2011 and 2006, respectively. Note the possible change in relative emission line ratios.

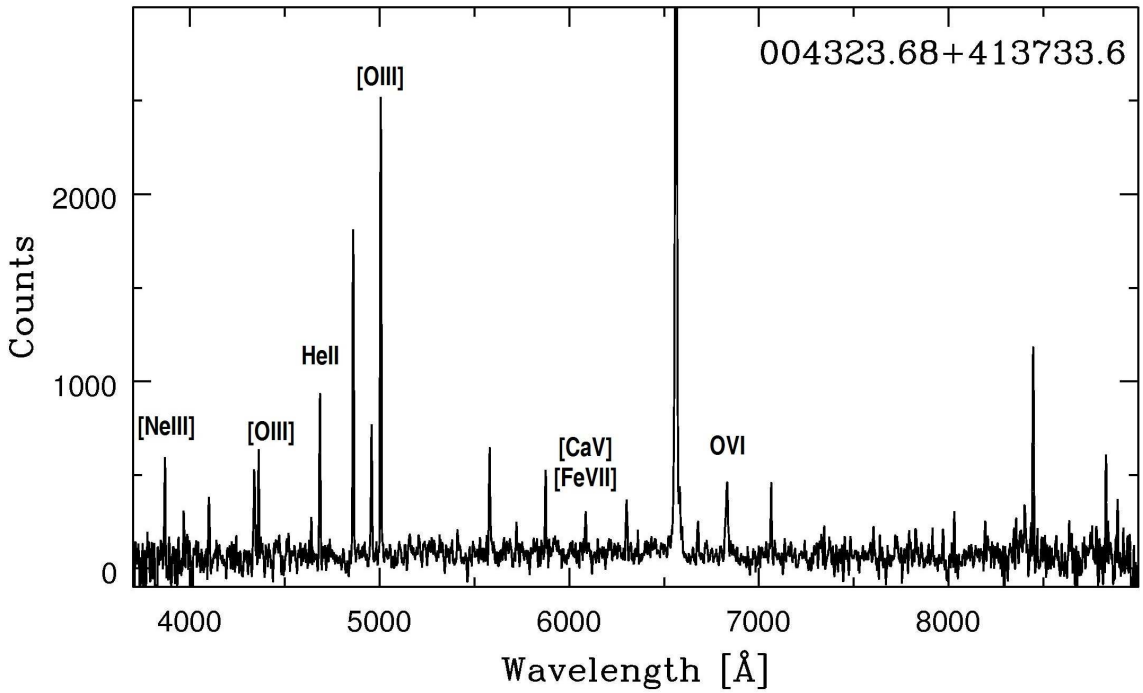

Figure 3. The spectrum of M31SyS J004323.68+413733.6. The symbiotic nature of this object is demonstrated by the presence of the broad Raman scattered O VI lines whereas the continuum is too weak to reveal any M giant features.

est IP emission lines visible in the spectrum, and where possible the spectral classification of the red giant.

Unfortunately, the above criteria are insufficient to detect D-type SySt unless they emit the Raman scattered O VI λ6830 (which is the case for only ~50 per cent of SySt). Nebulae around these D-type SySt look very much like genuine PNe because their Mira-type giants are, in most cases, embedded in warm dust shells, and the cool giant signatures are invisible in the optical spectra. The difference between the D-type SySt and PNe is, in principle, only detectable via near IR colours including the *JHKL* bands (e.g. Whitelock 1987; Schmeja & Kimeswenger 2001). The presence of the cool giant in an increasing fraction of these D-type SySt has

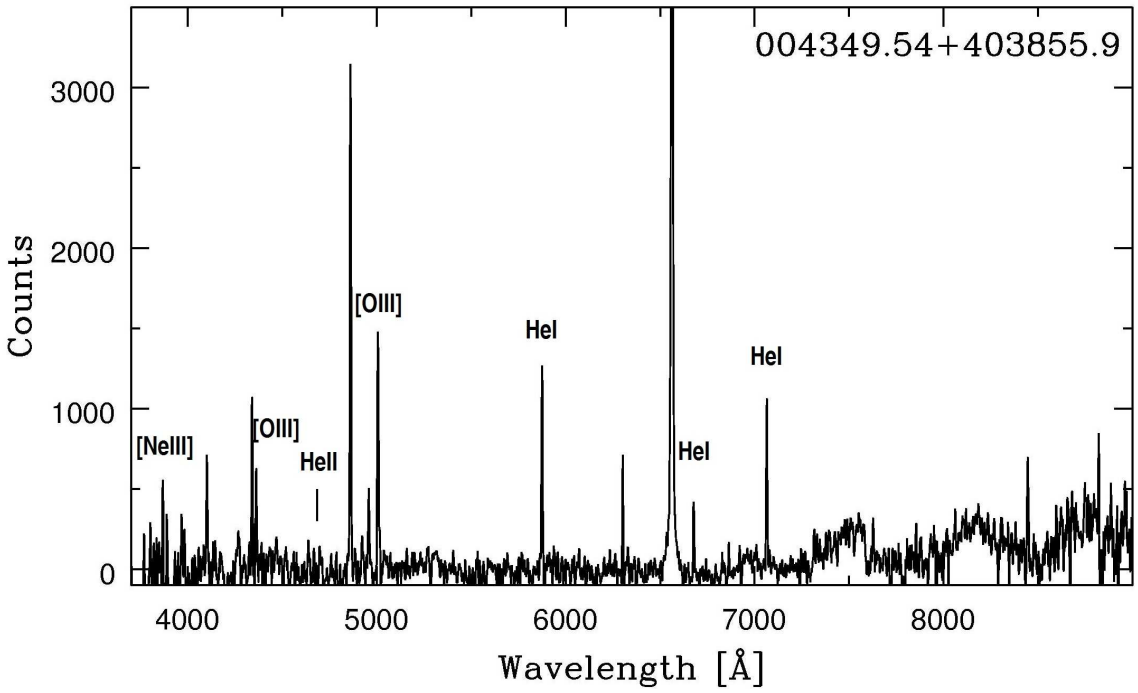

Figure 4. The spectrum of M31SyS J004349.54+413855.9 which is typical of a SySt with a lower ionization degree as indicated by the lack of measureable He II λ 4686 line.

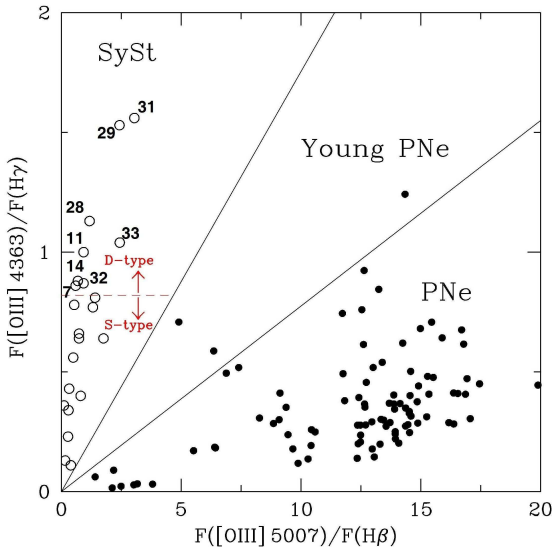

Figure 5. The M31 SySt together with the M31 PNe (Sanders et al. 2012) in the [O III] diagram. The two straight lines separate the regions occupied by SySt, young PNe and PNe (Gutierrez-Moreno et al. 1995). The dashed line represent the division line between the S- and D-types. Possible D-type candidates are identified by their ordinal numbers in Table 1.

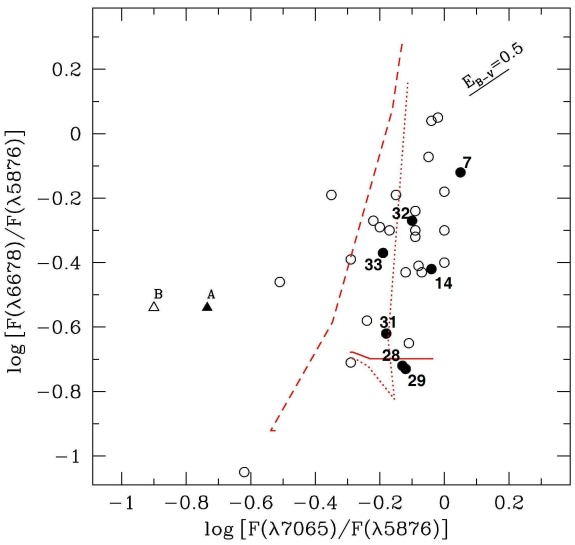

Figure 6. The M31 SySt in the He I diagram. The filled circles represent those SySt with [O III]/H$\beta \gtrsim 0.83$. The solid, dotted, and dashed lines represent the models for $T_e = 10^4$ K and $n_e = 10^6$, 10^{10}, and 10^{12} cm^{-3}, repectively (table 5 of Proga et al. 1994).

been confirmed by detection of Mira-type pulsations in their *JHKL* light curves (Whitelock 1987; Gromadzki et al. 2009).

Gutierrez-Moreno et al. (1995) demonstrated that a diagnostic diagram based only on the [O III] lines at 5007 and 4363 Å effectively separates SySt from planetary nebulae. It also distinguishes S- and D-type SySt from each other. We plotted the new M31 SySt together with the PNe in M31 (Sanders et al. 2012) in this diagram in Fig. 5. The new M31 SySt all lie exactly in the region occupied by SySt, whereas the M31 PNe fall into the region of PNe defined by Gutierrez-Moreno et al. (1995). Similarly, Proga et al. (1994) show that the He I $\lambda\lambda$5876, 6678 line ratio distinguishes between S- and D-type SySt in that $F(\lambda 6678)/F(\lambda 5876) \gtrsim 0.5$ for S-types and $F(\lambda 6678)/F(\lambda 5876) \sim 0.25$ for D-types. The He I diagram for our new SySt is presented in Fig. 6. Based on the locations of these objects in these two diagrams we estimate their IR types (Table 4). Those SySt with [O III]/H$\beta \gtrsim 0.83$, i.e. located in Fig. 5 above the division line between the S-

and D-types, are plotted as filled circles. We classified as D-type only 4 of these objects: M31SyS J004421.89+415125.6 (but see discussion of this object in Sect. 4.3), M31SyS J004432.09+411940.8, and M31SyS J004440.50+412052.2, and possibly M31SyS J004445.03+414156.5. The position of M31SyS J004021.10+404501.1 in Fig. 6 indicates that it is almost certainly S-type. This classification is, however, only provisional and should be confirmed by near IR observations. In the case of some objects, located in both diagrams near the dividing line between S- and D-types, the classification is very uncertain or impossible.

The absorption features of a cool component are present in most of the sample. Their spectral types (listed in Table 3) were mostly identified based on the depths of the heads of strong TiO bands at $\lambda\lambda$7054, 7589, and 8432, and in some cases the VO band at λ7845. The TiO bands seem to be present for some objects, but their under-exposed continua or spectra, contaminated by features of the surroundings due to poor background subtraction, make the spectral type estimate impossible. We note this by classifying their red components as 'M'.

The majority of our new SySt sample show the He II λ4686 emission line (26 out of 31), and many of them also show the Raman-scattered O VI lines (17 out of 31) and [Fe VII] $\lambda\lambda$5721, 6089 (10 out of 31). The highest ionization emission line detected is coronal [Fe X] λ6375 in M31SyS J004233.17+412720.7 and M31SyS J003846.16+400717.0, strongly suggesting that these SySt may be supersoft x-ray sources (see Sect. 4.3).

4 CHARACTERIZATION OF THE NEW SySt IN M31

We searched for matches to all new and possible SySt in all catalogs available in the CDS database via VizieR[2]. Table 1 lists all matches within 0.5 arcsec radius. 24 objects are listed by Azimlu et al. (2011) in their the catalogs of H II regions and PNe. They also provide estimates for the observed Hα fluxes (see Table 3), the M31 interstellar extinction, and the extinction-corrected total Hα luminosity, L(Hα) (see also Sect. 4.1).

Six objects coincide at the 0.2–0.5 arcsec level with the long period variables found by POINT-AGAPE survey of M31 (An et al. 2004). These coincidences seem to be real. The periods quoted in the POINT-AGAPE Catalogue (PAC) for these SySt, $P \sim$ 300–1000 days, fall in the range covered by the orbital periods of known SySt (Mikołajewska 2012). These are often classified as semiregular long-period variables because of their complex photometric behaviours (both components can be intrinsic variables). Several SySt also have matches in the catalogues of Vilardell et al. (2006). We briefly discuss these and some other noteworthy individual objects in Sect. 4.3.

4.1 Physical parameters

The physical parameters of the SySt sample are given in Table 4. To estimate the hot component temperature, $T_{\rm h}$, we employed the simple formula of the form $T_{\rm h}$[1000 K]=$IP_{\rm max}$[eV], where $IP_{\rm max}$ is the highest observed ionization potential (Mürset & Nussbaumer 1994). The accuracy of this method is ~10 per cent provided that the highest ionization stage is indeed observed. Since the highest ionization stages easily observed in the optical spectra of SySt are those of Fe^{+6} and O^{+5}, this method fails for $T_{\rm h} \gtrsim 115\,000$ K. The method also fails for S-type SySt with small and dense nebulae, and with $54\,000\,{\rm K} \gtrsim T_{\rm h} \lesssim 115\,000$ K because of the lack of strong permitted lines corresponding to the highest IP in this temperature range whereas the forbidden emission lines are either faint or absent due to high nebular density. Therefore we set the upper limit for $T_{\rm h}$ by the He II4686/Hβ ratio, and assuming case B recombination and cosmic He/H.

The interstellar reddening values, $E(B-V)$, were either adopted from Azimlu et al. (2011) or estimated from the H I and He I recombination lines. Unfortunately, in S-type SySt as well as some D-types, there are significant departures from case B conditions due to self absorption effects, and the reddening-free Balmer decrements are very steep with Hα/H$\beta \sim$ 5–10 (e.g. Proga et al. 1996). Similarly, the He I line ratios are affected by both optical depth and collisions, especially in S-type SySt (e.g. Proga et al. 1994, and references therein). Thus the $E(B-V)$'s in Table 4 were estimated using results of Netzer (1975) (H I) and Proga et al. (1994) (He I). Although their accuracy is not better than ~ 0.1, the differences between our estimates and the values quoted by Azimlu et al. (2011) in all but one case did not exceed 0.1. The absolute magnitudes were calculated assuming the distance to M31, m–M=24.47, corresponding to d=780 kpc (Vilardell et al. 2006), and extinction-corrected. Whenever possible, the extinction-corrected total Hα luminosity, L(Hα), is also given in Table 4.

The Hα total luminosity, and the absolute U magnitude ($M_{\rm U}$) characterize the nebular emission which is related to the hot component luminosity and temperature. Thus it is not surprising that there is some positive correlation between these two quantities. The absolute I magnitude ($M_{\rm I}$) characterizes the cool star in S-type SySt. In the case of dust obscured symbiotic Miras (D-types), their I magnitudes may not be representative of their intrinsic brightnesses, and in the most extreme cases, they can be dominated by the nebular emission. Although there is not sufficient information about the near-IR $JHKL$ colours for our M31 SySt, their PHAT $m_{814} - m_{160}$ colours, whenever available, seem to be consistent with cool stellar photospheres rather than warm dust emission. Therefore the correlation between L(Hα) and $M_{\rm I}$ (Fig. 7) indicates that there may be some relation between the hot component luminosity and that of the cool component. Such an effect is also observed in Galactic SySt (Fig. 7). Moreover Mikołajewska et al. (1997) found a relation between the hot component luminosity and the spectral class of the cool giant in the sense that the brightest hot components are the companions of the coolest and the most luminous M giants.

4.2 Comparison of the M31 SySt with those in our own Galaxy

In the following section, we compare the M31 sample with the SySt in the Milky Way. To calculate the Hα total luminosity, L(Hα), and the absolute U and I magnitudes, $M_{\rm U}$ and $M_{\rm I}$ for the galactic SySt, we collected the available relevant information. In particular, the the Hα fluxes for various samples of SySt were published by: Blair et al. (1983), Mikołajewska et al. (1997), Gutierrez-Moreno et al. (1999), and for individual SySt by: Kenyon & Fernandez-Castro (1987), Kenyon et al. (1991), Kenyon et al. (1993b), Brandi et al. (2005), Mikołajewska & Kenyon (1992), Schmid & Schild (1990). Most of these papers also contain information about the interstellar reddening, $E(B-V)$, and distances. Whenever different estimates for the same object were available, the $E(B-V)$'s were critically revised by one of us (JM). The $UBVI$ photometry was taken from

[2] http://vizier.u-strasbg.fr/viz-bin/VizieR

Table 3. Emission line ratios (Hβ=100), and the ion with the highest ionization potential observed in the spectra of the new M31 SySt. In addition, the last column gives the observed H_α fluxes taken from Azimlu et al. (2011) catalog.

M31SyS J	Hα	Hγ	Hδ	He II λ4686	[O III] λ4363	[O III] λ5007	[Fe VII] λ6086	O VI λ6830	He I λ5876	He I λ6678	He I λ7065	Ion	F(Hα)[3]
Symbiotic stars													
003846.16+400717.0	710	27	13	101				47	19	9		Fe^{+9}	
003857.17+403132.2	874	18	5		2	4			16	6	12	C^{+4}	4.35
003932.01+401224.7	742	25	8	44	9	11	4	43	27	13	22	O^{+5}	
003951.85+402153.8	562	27	12	15		64			34	17	23	He^{+2}	1.08
004005.96+401604.3	736	25	11	52		11		20	22	24	20	O^{+5}	
004021.10+404501.1	887	49	30	43	42	60			30	23	34	He^{+2}	4.49
004059.40+405003.1	638	35	24	66	14	81	27	52	6			O^{+5}	1.77
004117.11+404524.1	983	36	24	50	23	74		28	18	9	18	O^{+5}	4.99
004147.71+405737.1	601	39	27	25		40			52	21	26	He^{+2}	0.71
004155.61+410846.7	566	54			54	93			48	22		O^{+2}	0.81
004156.21+410735.0	825	56		110	44	54	13	43	47	9	24	O^{+5}	3.22
004216.70+404415.7	454	45	36	8		27			23	8	7	He^{+2}	1.99
004233.17+412720.7	1064	30	26	103	26	69	28	35	43	16	39	Fe^{+9}	2.40
004235.59+410148.0	841			80		144			65	33	41	He^{+2}	0.69
004241.96+415656.4	452	46	32		32	176			19	5	11	Ne^{+2}	
004319.98+415137.5	527	30	18	41	15			34	30	16	18	O^{+5}	
004323.68+413733.6	1115	27	16	50	21	132	17	51	28	14	23	O^{+5}	4.29
004334.79+413447.9	716	29	18		10	30			31	20	14	Ne^{+2}	2.12
004335.01+414358.2	429	42	32		34	104			32	27	29	Ne^{+2}	0.88
004349.54+413855.9	572	31	22		17	50		5	38	14	32	Ne^{+2}	
004353.59+415323.3	528	38	23	47	4	16	20		17	11	12	Fe^{+6}	2.56
004358.20+412850.9	403	55	19	11		12			23	26	22	He^{+2}	0.85
004359.52+410253.5	553	47	34	116				46	12		10	O^{+5}	1.05
004411.71+411336.0[1]	1133	26	14	57	11	33	1	74	23	9	19	O^{+5}	8.61
004411.71+411336.0[2]	1017	45	29	84	30	74		85	27	6	21	O^{+5}	
004421.89+415125.6	576	37	24	12	42	118			53	10	39	He^{+2}	6.24
004432.09+411940.8	543	34	18	84	52	243	21	23	16	3	12	O^{+5}	1.88
004433.74+414402.8	639	35	18	31	8	28	7	2	28	16	23	O^{+5}	4.60
004440.50+412052.2	370	41	18	24	64	305			21	5	14	He^{+2}	1.00
004445.03+414156.5	1103	28	23	50	24	93		77	24	13	19	O^{+5}	
004521.55+412557.3	623	34	17	55	37	244	21	12	14	6	9	O^{+5}	
004534.07+413049.0	454	43	31	17		40			24	16	24	He^{+2}	1.73
Possible symbiotic stars													
003923.79+400543.4	733								34	3	8	He^{+}	
004237.49+403813.2	932	37	20						10	4	10	He^{+}	2.19
004322.50+413940.9	P Cyg profile											H^{+}	2.00
004545.41+412851.6	495	52	32									Fe^{+2}	2.97

[1] observed in November 2006

[2] observed in October 2011

[3] in units of 10^{-15} erg s^{-1} cm^{-2}

Munari et al. (1992), and also from the DENIS catalogue available in the CDS database via VizieR. Although the DENIS *I* filter and the Cousins *I* filter, used by Munari et al. (1992) and Massey et al. (2006), differ slightly in their pivot wavelengths, the resulting magnitudes differ by no more than 0.1–0.2, which is less than the intrinsic variability of the majority of symbiotic red giants (e.g. Gromadzki et al. 2013, Angeloni et al. 2014). For these galactic SySt we used the Hα fluxes, and *U* mag observed during quiescence. During optical outbursts of any type (Z And-type, high states of accretion-powered SySt, symbiotic novae; e.g. Mikołajewska 2003) the continuum is cooler, and *UBV* magnitudes much higher.

Figs. 8–10 compare the distribution of the Hα total luminosity and the absolute magnitudes, M_U and M_I, of the M31 and galactic SySt. Some of the galactic D-type SySt show surprisingly low M_I. This is because their Mira components are obscured by optically thick dust, and their *I* magnitudes do not represent their intrinsic brightnesses. These plots show that we are clearly sampling similar populations, but that we are incomplete in M31 for all but the most luminous SySt. With a targeted campaign, we should be able to detect objects down to log L(Hα) = 34.3 (the limit of the Azimlu et al. (2011) catalog), well below the peak in the MW, and thus allow a rigorous comparison between the populations in the two galaxies.

Finally, Frankowski & Soker (2009) claimed that the intrinsic luminosity function in [O III] λ5007 line of the galactic symbiotic nebulae (SyStNLF) have very similar cutoff luminosity and general shape to those of the planetary nebulae. Unfortunately, we cannot estimate the [O III] luminosity for our M31 sample because the

Table 4. Physical parameters of new SySt in M31

M31SyS J	IR Type	Sp Type	E(B-V)	Ion	T_h [10^3 K]	M_I	M_{814}	M_U	M_{336}	L(Hα)[2]
Symbiotic stars										
003846.16+400717.0	S	M4	0.2	Fe^{+9}	235÷320	-4.1				
003857.17+403132.2	S	M4	0[1]	C^{+4}	64	-4.6		-4.5		3.18/83
003932.01+401224.7	S	M5	0.3	O^{+5}	114÷160	-4.6				
003951.85+402153.8	S	M3	0.17[1]	He^{+2}	54÷100	-4.2				1.18/30
004005.96+401604.3	S	M5/6	0.2	O^{+5}	114÷170	-5.1				
004021.10+404501.1	S	M	0.20[1]	He^{+2}	54÷160	-4.4		-2.9		5.22/136
004059.40+405003.1	S	M	0.21[1]	O^{+5}	114÷200	$\gtrsim$-3.9				2.10/57
004117.11+404524.1	S		0.2	O^{+5}	114÷170	-4.0		-4.1		5.82/143
004147.71+405737.1	S	M	0.3	He^{+2}	54÷125	-4.5				1.04/27
004155.61+410846.7		M	0.09[1]	O^{+2}	35	-4.8		-4.1		0.74/19
004156.21+410735.0		M	0.02[1]	O^{+5}	114÷360	-4.0				2.56/66
004216.70+404415.7	S	M	0[1]	He^{+2}	54÷90	-5.1		-3.5		1.46/38
004233.17+412720.7	S	M4	0.22[1]	Fe^{+9}	235÷320	-5.1				2.95/77
004235.59+410148.0	S	M	0.53[1]	He^{+2}	54÷240	-5.0				1.75/46
004241.96+415656.4	D:			Ne^{+2}	41					
004319.98+415137.5	S	M4	0	O^{+5}	114÷155	-4.5				
004323.68+413733.6	S		0.24[1]	O^{+5}	114÷170	-4.0				5.48/143
004334.79+413447.9	S	M	0.18[1]	Ne^{+2}	41	-5.3	-5.4	-4.7	-4.5	2.35/61
004335.01+414358.2	S	M4/5	0.2	Ne^{+2}	41					1.03/27
004349.54+413855.9	S	M5/6	0.2	Ne^{+2}	41	$\gtrsim$-3.8	-4.4		-4.1	
004353.59+415323.3	S	M6	0.11[1]	Fe^{+6}	100÷160	-4.1				2.43/64
004358.20+412850.9	S	M	0.26[1]	He^{+2}	54÷100	$\gtrsim$-3.9	-3.9		-1.8	1.15/30
004359.52+410253.5	S	M4/5	0.1	O^{+5}	114÷300	-4.1				0.97/25
004411.71+411336.0	S	M4/6	0.11[1]	O^{+5}	114÷260	-5.5	-5.2	-4.0	-3.8	8.26/216
004421.89+415125.6	D	M	0.3	He^{+2}	54÷100	-5.2		-5.6		9.5/243
004432.09+411940.8	D		0.23[1]	O^{+5}	114÷260	-3.3	-3.6	-4.2		2.73/71
004433.74+414402.8	S	M4	0	Fe^{+6}	100÷145	-5.3	-4.6	-3.5	-2.6	3.37/88
004440.50+412052.2	D		0.21[1]	He^{+2}	54÷125		-2.6		-4.0	1.21/32
004445.03+414156.5	S	M5	0.4	O^{+5}	114÷170	-4.9	-3.8	-4.7	-5.2	
004521.55+412557.3	D		0.5	O^{+5}	114÷180		-2.1		-4.5	
004534.07+413049.0	S		0.1	He^{+2}	54÷110	-5.1	-5.0	-4.4	-4.2	1.60/42
Possible symbiotic stars										
003923.79+400543.4		M	0	He^{+}	25	-4.8		-3.8		
004237.49+403813.2		M	0.5	He^{+}	25	-4.1		-4.4		5.10/132
004322.50+413940.9		M	0.40[1]	H^{+}	14	-6.1		-5.7		3.79/99
004545.41+412851.6		M3/5	0	Fe^{+2}	16	-5.4		-4.5		2.18/57

[1] adopted from Azimlu et al. (2011)

[2] in units of 10^{35} erg s^{-1}/L$\odot$

fiber spectra do not have absolute flux calibration. Nevertheless, the relative [O III] 5007/Hα fluxes for majority of our M31 SySt are lower than $\sim$ 0.1, and they never exceed 1. This fact combined with the total Hα luminosity indicates that the [O III] luminosity is much lower than the PN "universal" bright cutoff. In particular, the most luminous D-type SySt in our sample have L([O III]) 66, 39, and 32 L$\odot$, respectively, which is at least an order of magnitude lower than the value of the cutoff, L([O III]) $\simeq$ 600 L$\odot$, reported by Frankowski & Soker (2009).

4.3 Notes on some individual objects

4.3.1 M31SyS J004147.71+405737.1

Shafter & Irby (2001) reported an optical nova, M31N 1993-05, $\sim$ 1.5 arcsec away from M31SyS J004147.71+405737.1. However, their nova position's accuracy is, at best, $\sim$ 1 arcsec, and the putative nova and our SySt may well be the same object. M31N 1993-05, with its $m_{H\alpha}$ = 18.9, was one of faintest nova candidates in their survey. Taking into account their Hα filter width, $\Delta\lambda$=70 Å, and that $m_{H\alpha}$ = 0 for F(Hα)=1.77 $\times$ 10^{-7}erg cm^{-2} s^{-1}, we estimated F(Hα)=4.9 $\times$ 10^{-15}erg cm^{-2} s^{-1} for the nova. This is only 7$\times$ higher than F(Hα)=7.1 $\times$ 10^{-16}erg cm^{-2} s^{-1} measured for M31SyS J004147.71+405737.1 between 2000 August and 2002 September by Azimlu et al. (2011). If the coincidence between M31SyS J004147.71+405737.1 and M31N 1993–05 is real, then it was a Z And-type symbiotic outburst rather than a real thermonuclear nova. There is also a red variable, [PAC] 61099, only 0.16 arcsec away from our position of M31SyS J004147.71+405737.1, and the reported P $\sim$ 900^d (An et al. 2004) is consistent with the orbital periods observed for galactic S-type SySt, including those with the Z And-type outburst activity (Mikołajewska 2012).

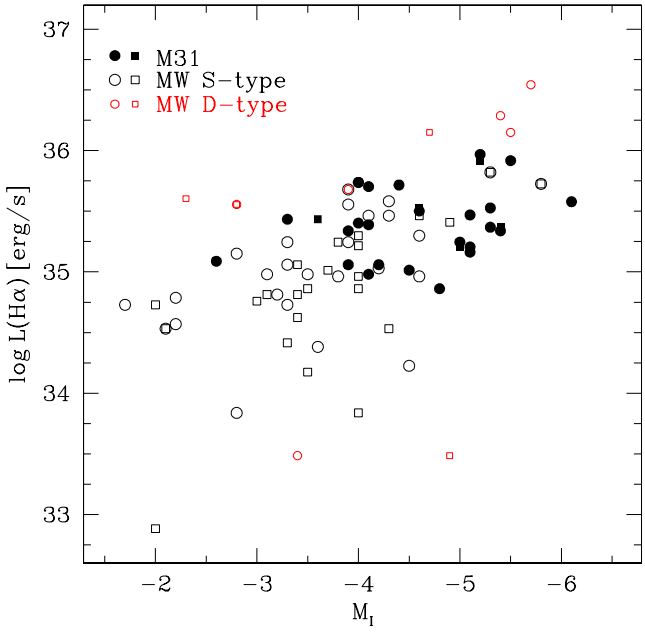

Figure 7. The Hα total luminosity vs. $M_{\rm I}$ for the M31 (filled symbols) and those in Milky Way (open symbols).

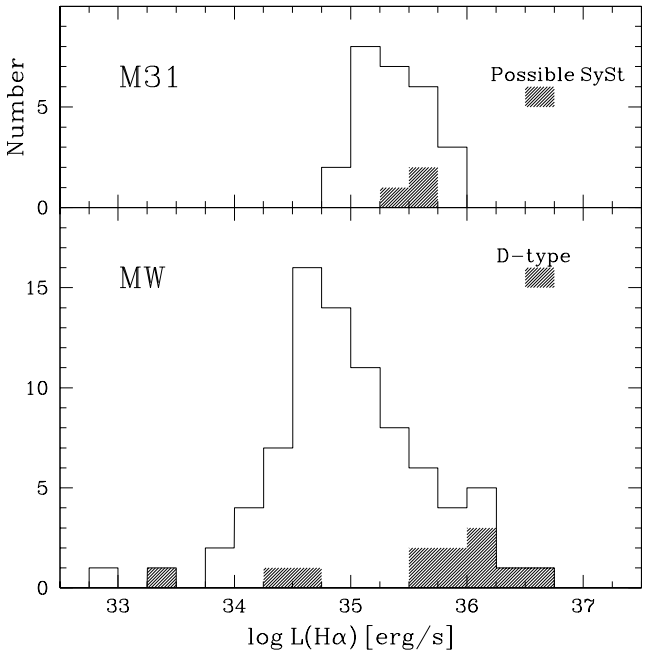

Figure 8. The Hα total luminosity, L(Hα), distribution. The values for the M31 SySt are from Azimlu et al. (2011) catalog; those for the galactic SySt - see text

4.3.2 *M31SyS J004216.70+404415.7*

This object has a very close 2MASS J00421671+4044158 counterpart ($\lesssim$ 0.2 arcsec). The 2MASS *JHK* combined with the LGGS *I* are then consistent with an un-reddened M giant. In addition, there is a red variable, [PAC] 57435 $\lesssim$ 0.3 arsec), with $P \sim 720^{\rm d}$, which seems to be the same object. The near IR colours and the period are then consistent with an S-type SySt.

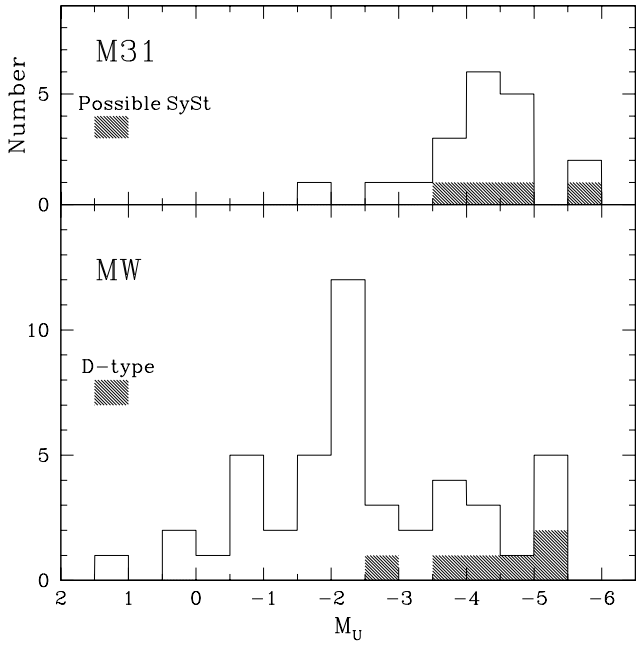

Figure 9. The absolute magnitude,M_U, distribution.

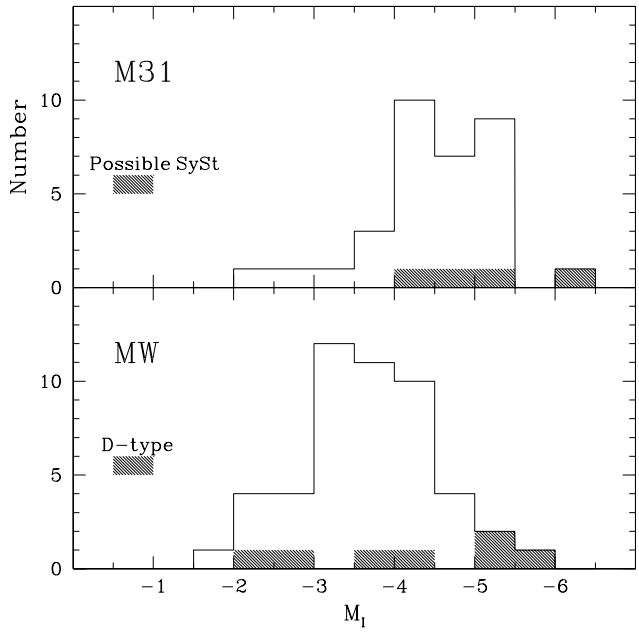

Figure 10. The absolute magnitude,M_I, distribution.

4.3.3 *M31SyS J004233.17+412720.7*

The most exceptional property of this object is the presence of very strong coronal [Fe x] λ6374, and [Fe ix] λ7892 emission lines, that combined with the fairly strong Raman scattered O vi, and [Fe vii] emission lines (Fig. 11) places M31SyS J004233.17+412720.7 amongst those SySt with the highest degree of ionization. The [Fe x] is observed in some classical novae (e.g. McLaughlin 1953), and symbiotic recurrent novae (Williams et al. 1991) during their nebular phase, but it is extremely rare in classical SySt. In principle, the presence of this line is well-documented only in SMC 3 which is also the most luminous supersoft X-ray source (SSXS) associated

with a SySt (e.g. Jordan et al. 1996, Orio et al. 2007), however, it is not as strong as in M31SyS J004233.17+412720.7 ([Fe x]/Hβ ~ 0.5 in SMC3, and ~ 3 in M31SyS J004233.17+412720.7). A weak [Fe x] was also reported in V2116Oph/GX1+4, the famous SySt with a neutron star accompanied by an M6 giant (Davidsen et al. 1977), and recently also in the C-rich SySt 2MASS J16003761–4835228 (Miszalski & Mikołajewska 2014).

Among our new M31 SySt, this emission was detected in only one other object – M31SyS J003846.16+400717.0 (Fig. A1). There is no X-ray counterpart to M31SyS J004233.17+412720.7 and any other of our new SySt. The nearest Chandra source, [VG2007] 257, is about 15 arsec away from M31SyS J004233.17+412720.7. This does not mean that the SySt does not produce any X-ray emission, as such emission could be absorbed locally (by the red giant wind), and/or by the interstellar medium. There is a bright red giant, 2MASS J00423313+4127207, ~ 0.4 arcsec away from the position of the SySt. Assuming that it is the cool component of M31SyS J004233.17+412720.7, the 2MASS *JHK* colours are consistent with a moderately reddened, $E(B-V)$ ~ 0.4, M4 giant. However, the $I-K$ ~ 4.3 would then be too red for such a star. One cannot, however, exclude that the spectral type is in fact later, and/or the star is variable.

4.3.4 M31SyS J004235.59+410148.0

There is a red variable, PAC] 93855, with P ~ 560$^{\rm d}$, ~ 0.5 arcsec away. The field is rather crowded, with a few other objects with similar I mag, and this may be an accidental coincidence.

4.3.5 M31SyS J004322.50+413940.9

The spectrum of this object, presented in Fig. 12, shows a very rich, low-excitation emission line spectrum, including H I, numerous Fe II and [Fe II], and Na I D, and very strong Ca II T lines. The H I and other permitted lines show P Cyg profiles with absorption component blue-shifted by ~ 350 km s^{-1} with respect to the emission peak. In addition, the red giant presence is indicated by the TiO bands, and the rising continuum in the red spectral range. Such a spectrum is typical for SySt during their strong optical outbursts. In particular, the similarity between the emission line spectrum of M31SyS J004322.50+413940.9 and that of RX Pup during its optical outbursts (e.g. Swings & Klutz 1976; Mikołajewska et al. 1999, and references therein) is remarkable. The *UBV* colours and absolute magnitudes, as well as total Hα luminosity of these two objects are also very similar: $M_{\rm U}$ ~ −5.2 to –5.7, and ~ −5.7 and L(Hα) ~ 180 L$_\odot$, and ~ 100 L$_\odot$, in RX Pup and M31SyS J004322.50+413940.9, respectively.

The coincidences between the position of the SySt and 2MASS J00432249+4139409 (0.06 arcsec), M31V J00432248+4139408 (0.13 arcsec), BATC_004322.51+413941.1 (0.26 arcsec) and [PAC] 47174 (0.27 arcsec) are all real because there is no other bright object near enough to be the SySt. The *JHK* colours are consistent with a moderately reddened, $E(B–V)$ ~ 0.5, M4 giant. The presence of a red giant is also evident from the BATC spectral energy distribution. The ~900-day period reported by An et al. (2004) very likely represents orbital variation. The shorter period P ~ 80$^{\rm d}$ (Vilardell et al. 2006) may be due to low-amplitude semiregular (SR) pulsation of the red giant, which is very common in Galactic and MC SySt (Gromadzki et al. 2013; Angeloni et al. 2014).

4.3.6 M31SyS J004323.68+413733.6

The spectrum of this object (Fig. 3) has a very weak continuum, and its symbiotic nature is indicated only by the O VI Raman scattered lines, and other high ionization emission lines. However, M31 J00432365+4137335 is only $\lesssim$ 0.2 arcsec away, with V = 22.5 and B = 23.1 (Vilardell et al. 2006). It was also detected by WISE, and in addition there is the nearby red variable, [PAC] 47312, with P ~ 1000$^{\rm d}$. The WISE magnitudes and colours are consistent with those of a red giant star.

4.3.7 M31SyS J004334.79+413447.9

Vilardell et al. (2006) report a variable star, M31V J00433475+4134477, with V=20.95 and B=21.46 very similar to LGGS magnitudes of the SySt (Table 2), and with P ~ 83$^{\rm d}$ (the light curves could be interpreted as due to a SR variable) which they identified as the LGGS object. There is also a red variable, [PAC] 46291, with P ~ 260$^{\rm d}$, which could be the same object. The HST F814W image[3] does not show any other bright and red object so close to M31SyS J004334.79+413447.9 (all these objects are within $\lesssim$ 0.4 arcsec).

4.3.8 M31SyS J004411.71+411336.0

This object was observed in November 2006, and October 2011. The two spectra, shown in Fig. 2, do not show significant differences except for some change in relative emission line intensity ratios (e.g. He II4686/Hβ, [O III]/Hβ). These changes can reflect some orbitally related changes or be due to intrinsic variability of the hot component. A comparison of the PHAT magnitudes (table 2) with the blue and near IR magnitudes from BATC DR1 suggests that M31SyS J004411.71+411336.0 was ~ 1 mag brigher in the blue optical range during the BAT observations whereas its near IR brightness was more or less the same.

4.3.9 M31SyS J004421.89+415125.6

Vilardell et al. (2006) report a variable star, M31V J00442188+4151255, coinciding with the position of the SySt within ~ 0.1 arcsec, and with V=20.97, B=21.35, and low-amplitude variability with P ~ 80$^{\rm d}$ which is most likely due to SR pulsations of the red giant. This would then indicate that M31SyS J004421.89+415125.6 is not a D-type SySt as suggested by its position in the [O III] diagram.

4.3.10 M31SyS J004433.74+414402.8

Bonanos et al. (2003) report a variable red star (V=20.82; B=21.29, I=19.07), D31 J004433.7+414403.0, which they tentatively classify as Type II Cepheid. However, its red colour (V-I =1.75) and positional coincidence with the red giant 2MASS J00443374+4144032 suggest that it may be M31SyS J004433.74+414402.8, especially since there is no other nearby red object in the HST F814 image bright enough to be a match. The 34$^{\rm d}$-periodicity would then reflect a SR pulsation of the red component.

[3] http://www.cfa.harvard.edu/oir/eg/m31clusters/symb/symb.html

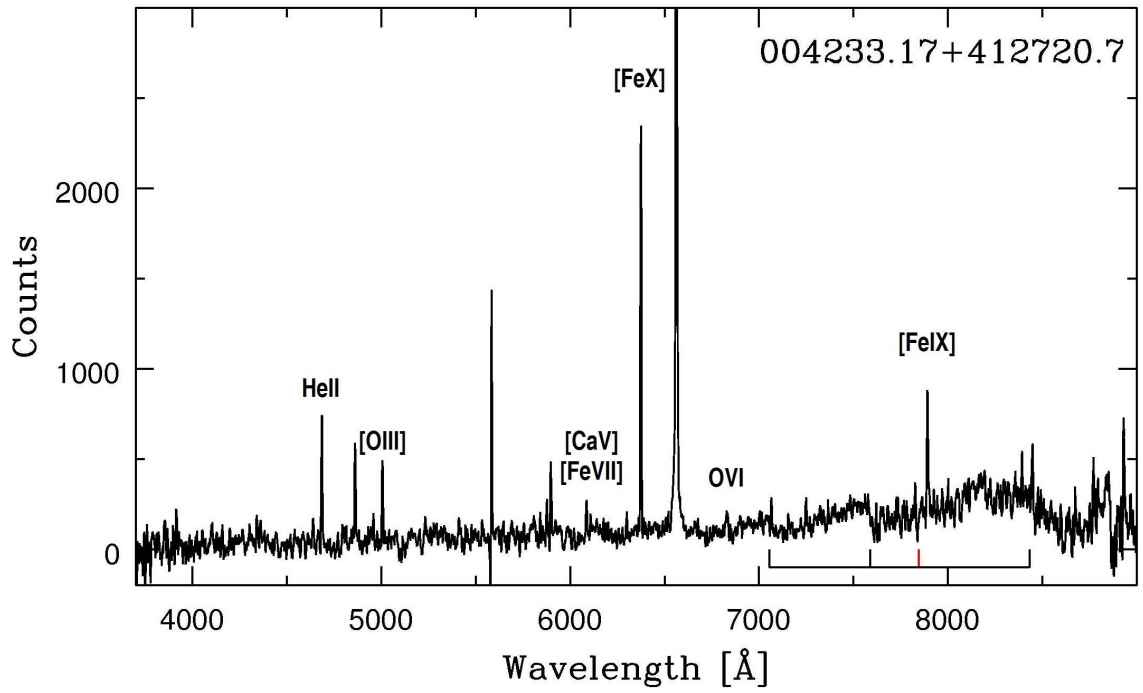

Figure 11. The spectrum of M31SyS J004233.17+412720.7, the SySt with the highest degree of ionization amongst all known SySt. The [Fe x] λ6374 and [Fe ix] λ7892 emission lines, and other high IP lines are indentified as well as the strongest molecular bands from the M giant.

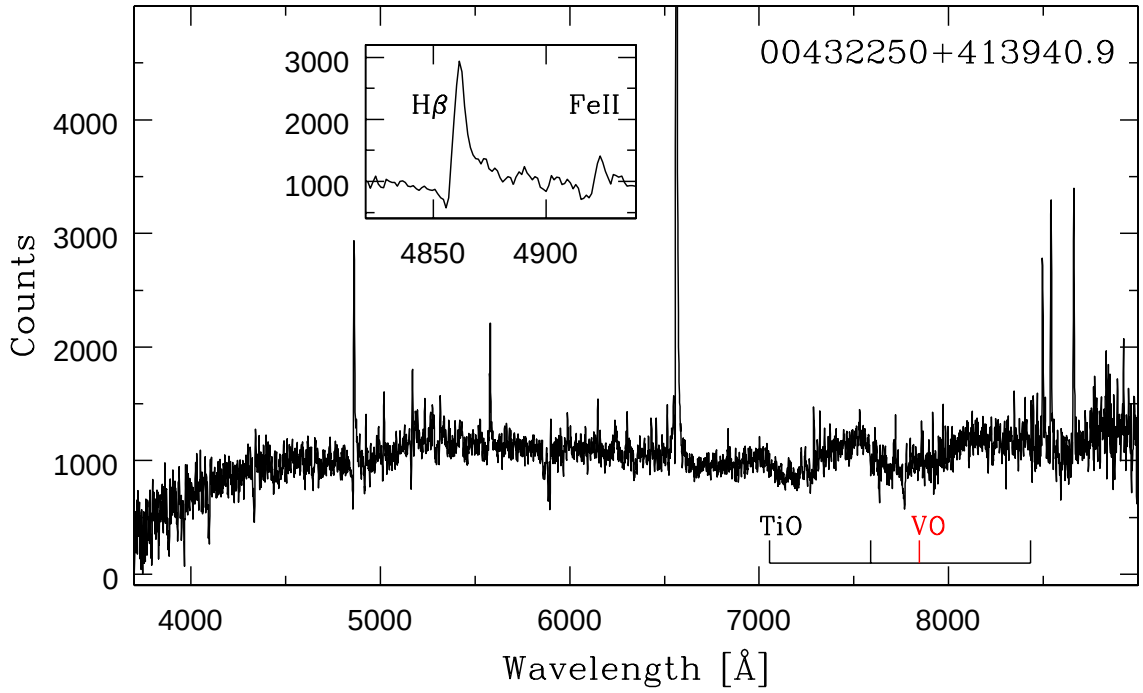

Figure 12. The spectrum of M31SyS J004322.50+413940.9, a possible SySt caught during an optical outburst.

4.3.11 M31SyS J004534.07+413049.0

Vilardell et al. (2006) report a variable star, M31V J00453405+4130487, with similar *BV* magnitudes and colour to those of the SySt, and $P \sim 80^{d}$ mostly likely due to SR variability of the red giant component.

5 CONCLUSIONS

We presented and discussed the first SySt detected in M31.

The main conclusions are as follows:

(i) A total of 31 SySt were confirmed. We tentatively identified 24 of them as S-types and 5 as D-types, however this classifica-

tion must be confirmed by near-IR photometry. 4 additional objects were classified as possible symbiotic stars.

(ii) A comparison of these new SySt with the galactic SySt indicates that we are sampling similar binary star populations, however, we are incomplete in M31 for all but the most luminous SySt.

(iii) M31SyS J004233.17+412720.7 was found to be the SySt with the highest ionization level among all known SySt.

(iv) Although M31SyS J004322.50+413940.9 was classified as a possible SySt, it is very likely that in 2006, when the Hectospec spectrum was taken, it was at an optical outburst maximum. Further observations are necessary to confirm its symbiotic nature.

More detailed spectral analysis of these new SySt will be the subject of a follow-up paper II.

6 ACKNOWLEDGMENTS

This study has been supported in part by the Polish NCN grant DEC-2013/10/M/ST9/00086. We gratefully acknowledge Nathan Sanders, for help with the emission line tables, and the fine support at the MMT Observatory, and The Local Group Galaxy Survey conducted at NOAO by Phil Massey and collaborators. MS thanks Allen Shafter for helpful details about M31N 1993–05. We also thank the referee, R. Corradi, for useful comments. This research has made use of the VizieR catalogue access tool, operated at CDS, Strasbourg, France.

REFERENCES

Angeloni R., et al., 2014, MNRAS, 438, 35
Allen D.A., 1980, MNRAS, 190, 175
Allen D.A., 1984, Proc. Astron. Soc. Australia, 5, 3
An, J.H, et al., 2004, MNRAS, 351, 1071
Azimlu, M., Marciniak, R., Barmby, 2011, AJ, 142, 139
Belczyński, K., Mikołajewska, J., Munari, U., et al., 2000, A&AS, 146, 407
Blair W. P., Feibelman W. A., Michalitsianos A. G., Stencel R. E., 1983, ApJS, 53, 573
Bonanos A. Z., Stanek K. Z., Sasselov D. D., Mochejska B. J., Macri L. M., Kaluzny J., 2003, AJ, 126, 175
Brandi E., Mikołajewska J., Quiroga C., Belczyński K., Ferrer O. E., Garcia L. G., Pereira, C. B., 2005, A&A, 440, 239
Caldwell, N., Harding, P., Morrison, H., et al. 2009, AJ, 137, 94
Corradi, R. L. M. 2012, Balt. Astronomy, 21, 32
Dalcanton J. J., et al., 2012, ApJS, 200, 18
Davidsen, A., Malina, R., Bowyer, S., 1977, ApJ, 211, 866
Dilday B., et al., 2012, Sci, 337, 942
Di Stefano R., Orio M., Moe M., eds, 2013, Proc. IAU Symp. 281, Binary Paths to Type Ia Supernovae Explosions, Cambridge Univ. Press, Cambridge
Di Stefano R., 2010, ApJ, 719, 474
Fabricant D., et al., 2005, PASP, 117, 1411
Frankowski A., Soker N., 2009, ApJ, 703, L05
Goncalves D. R., Magrini L., Munari U., Corradi R. L. M., Costa R. D. D., 2008, MNRAS, 391, 84
Gromadzki, M., Mikołajewska, J., 2009, A&A, 495, 931
Gromadzki M., Mikołajewska J., Whitelock P. A., Marang F., 2009, Acta Astr., 59, 169
Gromadzki M., Mikołajewska J., Soszyński I., 2013, Acta Astr., 63, 405
Gutierrez-Moreno A., Moreno H., Cortes G., 1995, PASP, 107, 462
Gutierrez-Moreno A., Moreno H., Costa R., 1999, PASP, 111, 571
Hakobyan, A. A., et al., 2011, Astrophys,. 54, 301
Iben I., Tutukov A. V., 1984, ApJS, 54, 335
Jordan S., Schmutz W., Wolff B., Werner K., Mürset U., 1996, A&A, 312, 897
Kenyon S. J., Oliversen N. A., Mikolajewska, J., Mikolajewski M., Stencel R. E., Garcia M. R., Anderson C. M., 1991, AJ, 101, 637
Kenyon S. J., Fernandez-Castro T., 1987, ApJ, 316, 427
Kenyon S. J., Livio M., Mikołajewska J., Tout C. A., 1993, ApJL, 407, L81
Kenyon S. J., Mikołajewska J., Mikolajewski M., Polidan R. S., Slovak M. H., 1993, AJ, 106, 1573
Kniazev A. Y., et al., 2009, MNRAS, 395, 1121
Li, W., et al, 2011, Nature 480, 348
Magrini, L., Corradi, R. L. M., Munari, U. 2003, in Corradi, R. L. M., Mikołajewska, J., Mahoney, T., eds, Symbiotic Stars Probing Stellar Evolution, ASP Conf. Ser. Vol. 303, Astron. Soc. Pac., San Francisco, p.539
Massey, P., Olsen, K. A. G., Hodge, P. W., Strong, S. B., Jacoby, G. H.; Schlingman, W., Smith, R. C., 2006, AJ, 131, 2478
Massey, P., McNeill, R. T., Olsen, K. A. G., Hodge, P. W., Blaha, C., Jacoby, G. H., Smith, R. C., Strong, S. B. 2007, AJ, 134, 2474
McLaughlin D. B., 1953, ApJ, 118, 27
Merrett H. R., et al., 2006, MNRAS, 369, 120
Mikołajewska, J., 2003, in Corradi, R. L. M., Mikołajewska, J., Mahoney, T., eds, Symbiotic Stars Probing Stellar Evolution, ASP Conf. Ser. Vol. 303, Astron. Soc. Pac., San Francisco, p.9.
Mikołajewska J., 2007, Balt. Astronomy, 16, 1
Mikołajewska J., 2012, Balt. Astronomy, 21, 5
Mikołajewska J., 2013, in Di Stefano, R., Orio, M. and Moe, M., eds, Proc. IAU Symp. 281, Binary Paths to Type Ia Supernovae Explosions, Cambridge Univ. Press, Cambridge
Mikołajewska J., Kenyon S.J., 1992, AJ, 103, 579
Mikołajewska J., Acker A., Stenholm B., 1997, A&A, 327, 191
Mikołajewska J., Brandi E., Hack W., Whitelock P. A., Barba R., Garcia L., Marang F., 1999, MNRAS, 305, 190
Miszalski B., Mikołajewska J., 2014, MNRAS, 440, 410
Miszalski B., Mikołajewska J., Udalski A., 2013, MNRAS, 432, 3186
Miszalski B., Mikołajewska J., Udalski A., 2014, MNRAS, in press
Mochejska B., Kaluzny J., StaneK K. Z., Sasselov D. D., 2001, AJ, 122,1283
Munari U., Renzini A., 1992, ApJ, 397, 87
Munari U., Zwitter T., 2002, A&A, 383, 188
Munari U., Yudin B. F., Taranova O. G., Massone G., Marang F., Roberts G., Winkler H., Whitelock P. A., 1992, A&AS, 93, 383
Mürset U., Nussbaumer H., 1994, 282, 586
Mürset U., Schmid H. M., 1999, A&AS, 137, 473
Netzer H., 1975, MNRAS, 171, 395
Oliveira J.M., et al., 2013, MNRAS, 428, 3001
Orio M., Zezas A., Munari U., Siviero A., Tepedelenlioglu E., 2007, ApJ, 661, 1105
Paczynski B., 1985, in Cataclysmic variables and low-mass X-ray binaries; Proceedings of the Seventh North American Workshop, Dordrecht, D. Reidel Publishing Co., p.1
Proga D., Mikołajewska J., Kenyon S.J., 1994, MNRAS, 268, 213P
Proga D.Kenyon S.J., Raymond J.C., Mikołajewska J., 1996, ApJ,

471, 930
Sanders, N. E., Caldwell, N., McDowell, J., Harding, P. 2012, ApJ, 758, 133
Schaefer B., Pagnotta A., Nature 481, 164
Schmeja S., Kimeswenger S., 2001, A&A, 377, L18
Schmid H. M., 1989, A&A, 211, L31
Schmid H. M., Schild H., 1990, A&A, 246, 84
Schmid H. M., Schild H., 2002, A&A 395, 117
Shafter A. W., Irby B. K., 2001, ApJ 563 749
Shara M. M., Yaron O., Prialnik D., Kovetz A., 2010, ApJ 712, 143
Swings J. P., Klutz M., 1976, A&A, 46, 303
Vilardell, F., Ribas, I, Jordi, C., 2006, A&A, 459, 321
Webbink R. F., 1984, ApJ, 277, 355
Whitelock P.A, 1987, PASP, 99, 573
Williams R. E., et al., 1991, ApJ, 376, 721
Williams, B. F., Lang, D., Dalcanton, J. J., et al. 2014, ApJ, submitted
Yaron O., Prialnik D., Shara, M. M., Kovetz A., 2005, ApJ, 623, 398

APPENDIX A: HECTOSPEC SPECTRA OF THE M31 SySt AND POSSIBLE SySt

This paper has been typeset from a TEX/ LATEX file prepared by the author.

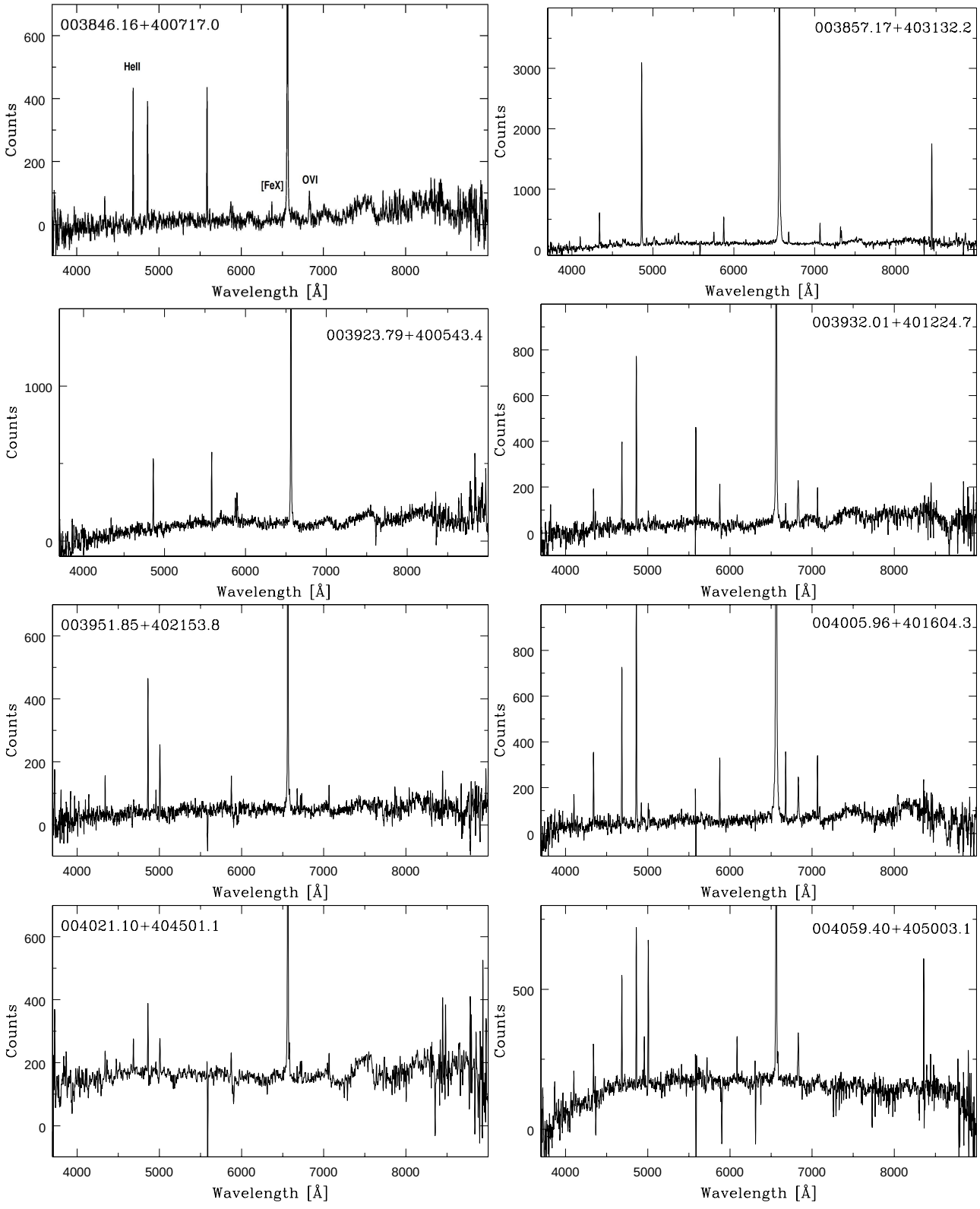

Figure A1. Spectra of SySt in M31

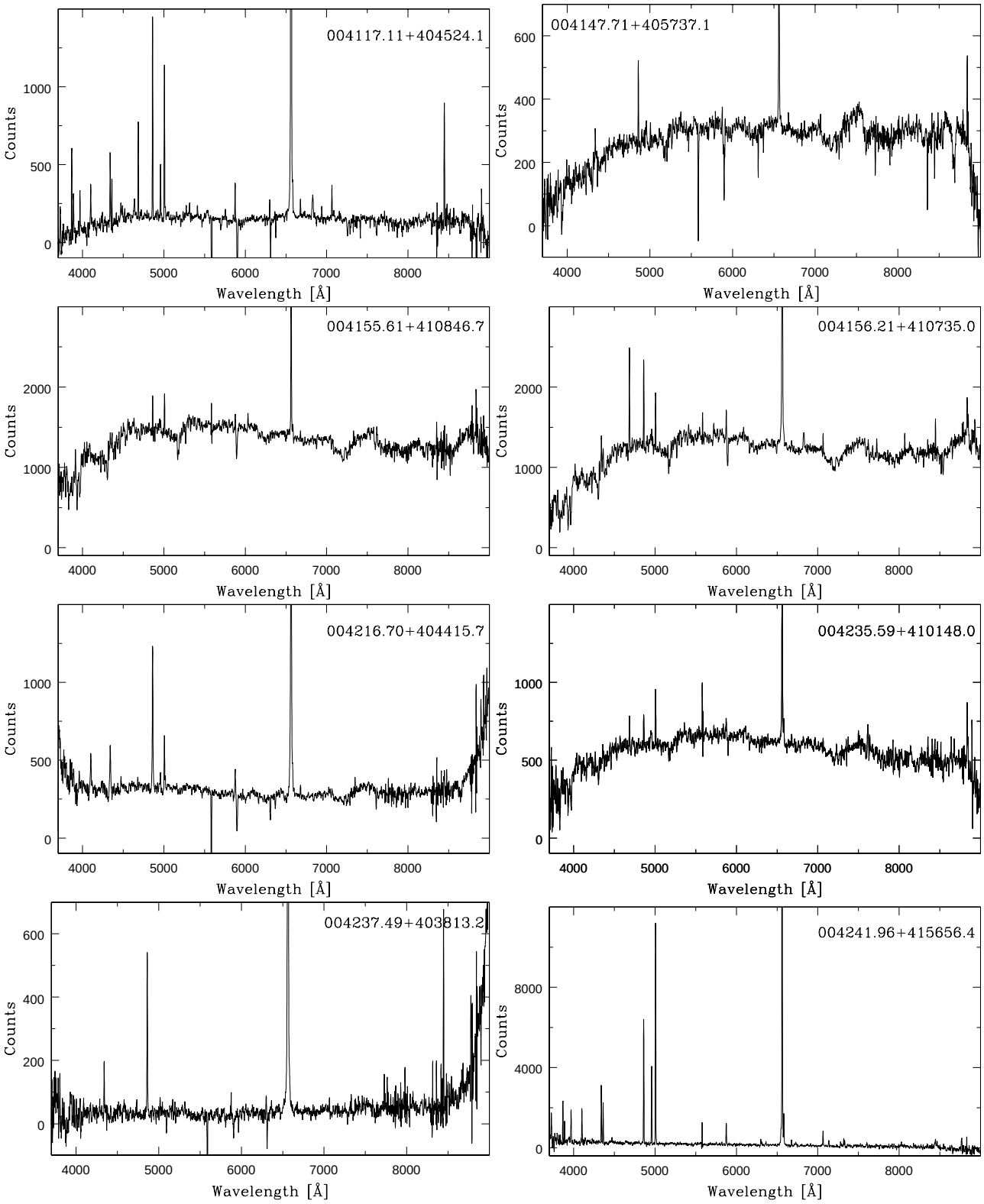

Figure A2. Spectra of SySt in M31

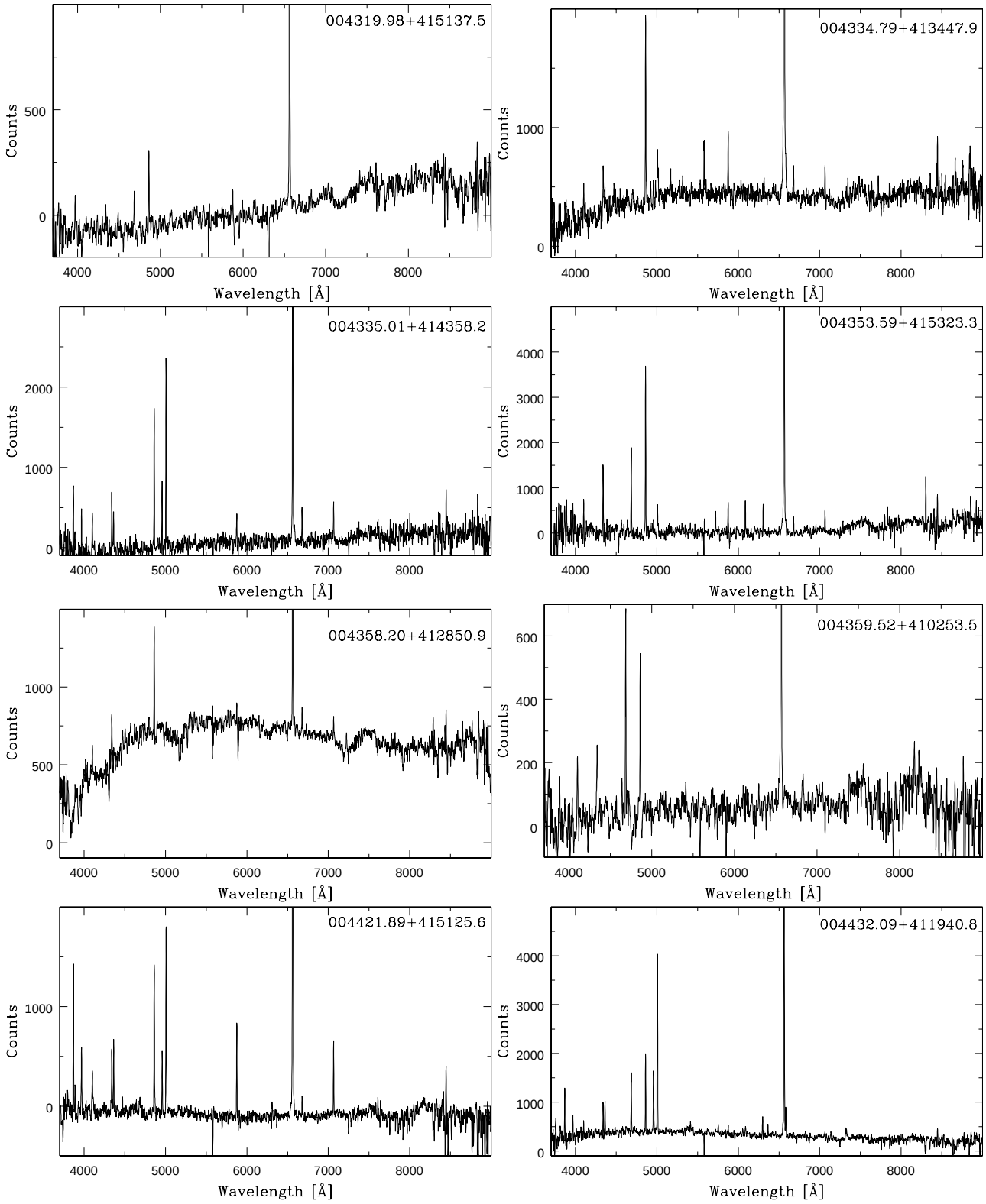

Figure A3. Spectra of SySt in M31

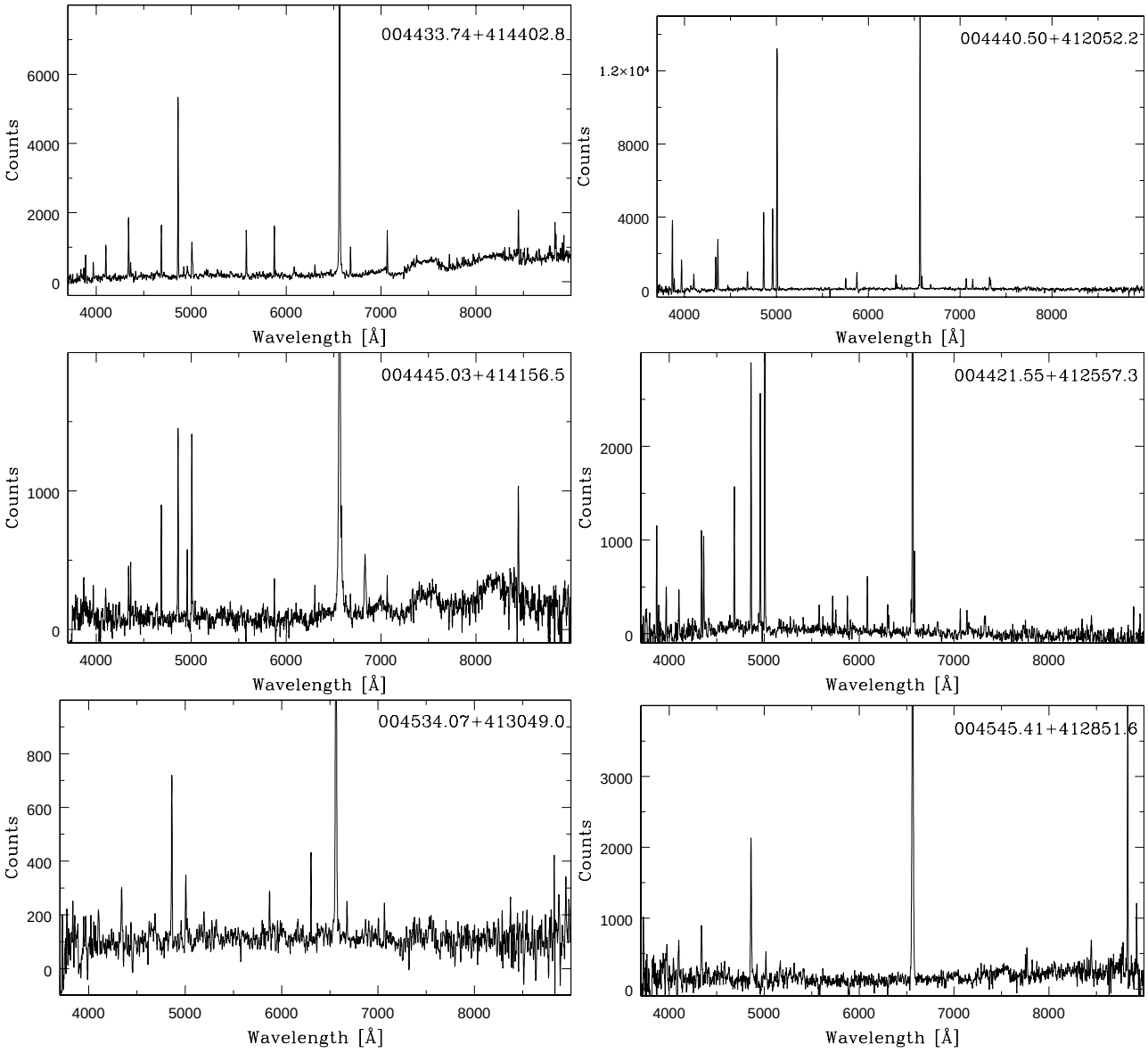

Figure A4. Spectra of SySt in M31